Carcinogenesis, 2021, Vol. 42, No. 6, 891–902

doi:10.1093/carcin/bgab035
Advance Access publication May 16, 2021
Original Article

ORIGINAL ARTICLE

PD-1 blockade prevents the progression of oral carcinogenesis

Yunmei Dong[†], Zhen Wang[†], Fei Mao, Luyao Cai, Hongxia Dan, Lu Jiang, Xin Zeng, Taiwen Li[*], Yu Zhou[*] and Qianming Chen

State Key Laboratory of Oral Diseases, National Clinical Research Center for Oral Diseases, Chinese Academy of Medical Sciences Research Unit of Oral Carcinogenesis and Management, West China Hospital of Stomatology, Sichuan University, Chengdu, China

[†]The authors contributed equally to this study and share the first authorship.
[*]To whom correspondence should be addressed. State Key Laboratory of Oral Diseases, National Clinical Research Center for Oral Diseases, Chinese Academy of Medical Sciences Research Unit of Oral Carcinogenesis and Management, West China Hospital of Stomatology, Sichuan University, No. 14, Section 3, Renmin South Road, Chengdu 610041, China. Tel: +86 18980754549; Fax: +86 85501484; Email: litaiwen@scu.edu.cn
Correspondence may also be addressed to Yu Zhou. State Key Laboratory of Oral Diseases, National Clinical Research Center for Oral Diseases, Chinese Academy of Medical Sciences Research Unit of Oral Carcinogenesis and Management, West China Hospital of Stomatology, Sichuan University, No. 14, Section 3, Renmin South Road, Chengdu 610041, China. Tel: +86 18980754549; Fax: +86 85501484; Email: 812471898@qq.com

Abstract

Oral squamous cell carcinoma (OSCC) is one of the most common malignancies in the head and neck with a poor prognosis. Oral cancer development is a multistep process involving carcinogenesis. Though significant advances in cancer immunotherapy over the years, there is lack of evidence for T-cell exhaustion during oral carcinogenesis. Clinical specimens from healthy donors and patients diagnosed with oral leukoplakia (OLK) or OSCC were collected for immunohistochemical staining with PD-L1, CD86, CD8, PD-1 and CTLA-4 antibodies. Meanwhile, chemically induced mouse models of oral carcinogenesis were constructed with 4-nitroquinolone-*N*-oxide induction. Exhaustion status of T cells was measured by flow cytometry for spleens and by multiplex immunohistochemistry for formalin-fixed paraffin-embedded lesions in multiple stages of oral carcinogenesis. The efficacy of PD-1 blockade with or without cisplatin treatment was evaluated on the mice in precancerous and OSCC stages. We observed higher expression of PD-1 in the human OLK and OSCC tissues compared with the normal, while low expression CTLA-4 in all oral mucosa tissues. Animal experiments showed that the exhausted $CD4^+$ T cells existed much earlier than exhausted $CD8^+$ T cells, and an increased ratio of stem-like exhausted T cells and partially exhausted T cells were detected in the experimental groups. Besides, the expression of immune checkpoint markers (PDCD1, CTLA4 and HAVCR2) was strongly positively correlated with cytokines (IFNG and IL-2). In summary, T-cell exhaustion plays a vital role in oral carcinogenesis, and PD-1 blockade can prevent the progression of oral carcinogenesis.

Introduction

Oral squamous cell carcinoma (OSCC) is one of the most common malignancies in the head and neck (1). The prognosis of OSCC is poor and the reported 5-year survival rate is about 63% in the USA (2). Most patients diagnosed with OSCC have experienced oral carcinogenesis, a multistage and multifocal process involving genetic changes of oral mucosa from the normal one to oral potentially malignant disorders, and finally to OSCC. Oral leukoplakia (OLK) is one of the most common oral potentially malignant disorders in the clinical practice of oral medicine. A systematic review of observational studies on OLK reported the estimated overall (mean) malignant transformation rate was 3.5%, with a wide range between 0.13 and 34.0% (3).

Received: December 12, 2020; **Revised:** April 14, 2021; **Accepted:** May 5, 2021

Abbreviations

HNSCC	head and neck squamous cell carcinoma
mIHC	multiplex immunohistochemistry
OLK	oral leukoplakia
OSCC	oral squamous cell carcinoma

T-cell exhaustion is a state of T-cell dysfunction with poor effector function, sustained expression of inhibitory receptors and a transcriptional state distinct from that of functional T cells (4). Recent studies found that exhausted T cells can be detected in the microenvironment of precancer diseases and tumors, which results in the forming of suppressive immune microenvironment (5–7). Inhibitory receptors, also called inhibitory immune checkpoints, are closely related to T cells' function, and they can control the intensity and duration of the immune response to ensure that T cells are not overstimulated (8). Additionally, the expression levels of inhibitory receptors can affect the degree of T-cell failure (9). Programmed cell death-1 (PD-1) and cytotoxic T-cell-associated antigen-4 (CTLA-4) are currently the most widely studied and used inhibitory receptors.

In recent years, there has been a great deal of interest in how to restore T cells' function to kill abnormal cells. Studies demonstrated that blocking a single inhibitory immune checkpoint or jointly blocking two inhibitory immune checkpoints can partially restore the biological function of T cells in some malignancies, such as melanoma, non-small-cell lung cancer and renal cancer (10–12). Anti-PD-1/programmed death-ligand 1 (PD-L1) immunotherapy has demonstrated success in the treatment of advanced head and neck squamous cell carcinoma (HNSCC), however, only a small number of patients with HNSCC can benefit from PD-1/PD-L1 blockade (13). Recent studies have found that the efficacy of PD-1 blockade can be reinforced by chemotherapy (14,15).

Oral mucosa gradually develops into epithelial hyperplasia during carcinogenesis. Evidence of exhausted T cells' role in oral carcinogenesis is still poor and it is unclear whether the progression of oral carcinogenesis could be delayed by PD-1 blockade combined with/without chemotherapy. To address these points, we collected human normal, OLK, OSCC specimens, and constructed 4-nitroquinolone-*N*-oxide (4-NQO)-induced mice models to simulate the whole process of oral carcinogenesis. Human specimens were used for immunohistochemistry. Tongues coming from mice were used for multiplex immunohistochemistry (mIHC) and spleens were used for flow cytometry. We found that exhausted T cells could be observed at the stage of precancer, and with the progression of oral carcinogenesis T cells demonstrated dynamic characteristics. Subsequently, based on previously constructed mice models, we introduced the treatment of PD-1 blockade with/without cisplatin in oral carcinogenesis. The results showed that PD-1 blockade could reduce the growth of OSCC obviously, and the efficacy could be reinforced by cisplatin. Our study provides a theoretical basis for the usage of PD-1 blockade to manage OLK or OSCC in clinical practice.

Methods

Patients and tissue samples

A total of 11, 26 and 53 normal oral mucosa tissues, OLK and OSCC tissues, respectively, were collected in the West China Hospital of Stomatology, Sichuan University. The demographic data and clinical features of the patients diagnosed with OLK or OSCC are presented in Supplementary Table 1, available at *Carcinogenesis* Online. Normal oral mucosal tissues were derived from patients undergoing teeth extraction, implantation or orthognathic surgery. OLK tissues originated from patients who had been diagnosed with OLK via biopsy. OSCC tissues were derived from patients who had been diagnosed with OSCC using pathology and had received surgical treatment. Consecutive sections were cut from the paraffin-embedded tissue specimens of all patients for immunohistochemical analysis. All tissue specimens were histologically diagnosed by pathologists. All patients' basic information and clinical and pathological data were collected for subsequent analysis. This study was approved by the West China Hospital of Stomatology Institutional Review Board (WCSHIRB-D-2016-173). All included patients provided written informed consent.

Immunohistochemistry and evaluation

The paraffin-embedded human tissue sections were used for immunohistochemical staining with anti-PD-L1 (ab205921, Abcam), anti-PD-1 (ab52587, Abcam), anti-CD86 (ab53004, Abcam), anti-CTLA-4 (ab237712, Abcam) and anti-CD8 (ab4055, Abcam) (Supplementary Figure 1A, available at *Carcinogenesis* Online). The immunostaining was visualized with the DAB Detection Kit (Gene Tech, China) using a peroxidase and diaminobenzidine substrate. The semi-quantitative fractionation method of Fromowite positive cells (yellow or brownish yellow particles appear as positive in the cell membrane and/or cell membrane) was used to evaluate the expression of PD-L1 in human tissues and the staining results were double-blindly read by two pathologists and quantified by Imagescope software (16). Each section was observed under a high-power microscope (×400); five fields of view were randomly selected, and the scores were allocated in terms of the intensity of staining and the proportion of positive cells in each field of view. If the scoring results were inconsistent, a third researcher made the final decision regarding the score. Based on the intensity of staining, the staining results were divided into four grades: 0 (no stain), 1 (light yellow), 2 (brown) and 3 (tan). Additionally, based on the proportion of positive cells, the staining results were divided into five grades: 0 points (0–4%), 1 point (5–25%), 2 points (26–50%), 3 points (51–75%) and 4 points (76–100%). The final result was the product of the two scores, which was divided into four levels: 0–3 points (negative), 4–5 points (+), 6–8 points (++), 9–12 points (+++), i.e. negative (–), weak positive (+), medium positive (++), strong positive (+++) (17).

Mice

Five-week-old female C57BL/6 mice ($n = 80$) were purchased from Chengdu DaShuo Animal Laboratory Company to construct animal models for OLK and OSCC. Mice were fed with tap water containing 100 μg/ml 4-NQO (Sigma–Aldrich) for 16 weeks and then changed with tap water. Two mice were killed at week 16 and 20 to ensure the successful construction of mice models. The study protocols were approved and performed following the guidelines of the West China Hospital of Stomatology Institutional Review Board (WCSHIRB-D-2017-205).

Treatment

Once the models for OLK were successfully constructed, the mice were randomly divided into two groups. Mice were then treated with anti-PD-1 (RMP1-14, BioXCell) (200 μg each, twice/week) or control Ig (2A3, BioXCell) (200 μg each, twice/week) by intraperitoneal injection. Mice were killed after a 4-week drug intervention.

After the models for OSCC were successfully constructed, the mice were divided into four groups according to tumor size. Mice were then treated with antibodies to PD-1 (RMP1-14, BioXCell) (200 μg each, twice/week) or/and cisplatin (*cis*-diamminedichloroplatinum (II): CDDP; 5 mg/kg, once/week), and the control group was injected with control Ig (2A3, BioXCell) (200 μg each, twice/week) by intraperitoneal injection (18). Mice weight and tumor sizes were measured weekly. Because the location of the lesion is on the tongue, it is impossible to measure the size of tumors with a vernier caliper. Therefore, we anesthetized the mice with isoflurane and measured the lesions with a periodontal probe. Mice were killed after a 4-week drug intervention (Supplementary Figure 1B, available at *Carcinogenesis* Online).

Hematoxylin and eosin (H&E) staining and evaluation

The paraffin-embedded mice tongue sections were used for hematoxylin and eosin (H&E) staining. The histopathological grades—none (without dysplasia), dysplasia, carcinoma—were performed with a light microscope (Olympus Optical) and reviewed by two experienced pathologists.

Flow cytometric analysis

Spleens were harvested from mice for flow cytometric analysis as described previously (19). After single-cell suspension being prepared successfully, red blood cell lysate (Beyotime) was used to lyse red blood cells. Cells were stimulated *in vitro* with 50 ng/ml phorbol 12-myristate 13-acetate (Sigma–Aldrich) and 1 mg/ml ionomycin (Sigma–Aldrich) for 4 h, and finally, monensin (10 μg/ml, Sigma–Aldrich) was added to allow for blocking for 2 h. After the stimulation was completed, the cell surface marker was stained; then the intracellular proteins and factors staining were performed after the cell membrane and the nuclear membrane were broken. For surface staining, immune cell suspensions were stained with BD Horizon™ V450 Rat Anti-Mouse CD45, BD Horizon™ BV510 Hamster Anti-Mouse CD3e, BD Pharmingen™ APC-Cy™7 Rat Anti-Mouse CD4, BD Pharmingen™ PE-Cy™7 Rat Anti-Mouse CD8a, BD Horizon™ PE-CF594 Hamster Anti-Mouse CD279 (PD-1), BD Pharmingen™ APC Rat Anti-Mouse CD274 (PD-L1), BD Horizon™ APC-R700 Hamster Anti-Mouse CD152 (CTLA-4) and BD Pharmingen™ PE Mouse Anti-Mouse CD366 (TIM-3). For intracellular proteins and cytokines were stained with BD BV650 Mouse Anti-T-bet, EOMES Monoclonal Antibody (Dan11mag, Alexa Fluor 488, eBioscience™), BD Horizon™ BV786 Rat Anti-Mouse IFN-γ, BD Horizon™ BV605 Rat Anti-Mouse IL-2, Brilliant Violet 421™ anti-mouse LAP (TGF-β1), BD Pharmingen™ PerCP-Cy™5.5 Rat Anti-Mouse Foxp3. Cells were acquired on the ZE5 (Bio-Rad) and analysis was conducted using FlowJo software. Flow cytometry gating strategies were as follows: Firstly, we identified $CD45^+$ cells, and then $CD3^+CD4^+$ cells $CD3^+CD8^+$ cells were gated. Finally, the subsets of $CD3^+CD4^+$ cells $CD3^+CD8^+$ cells were analyzed (Supplementary Figure 1C, available at *Carcinogenesis* Online).

Multiplex immunohistochemistry

The paraffin-embedded tongue tissues from mice were stained using the PerkinElmer OPAL 7-Colour Automation IHC kit and the following anti-mice antibodies: anti-CD4 (ab183685, Abcam), anti-CD8 (ab237723, Abcam) and anti-PD-1 (D7D5W, CST). Nuclei were stained with 4′,6-diamidino-2-phenylindole. The experiment was completed according to the recommended kit instructions.

TIMER and TISCH database analysis

The TIMER web server provides comprehensive analysis and visualization functions of tumor-infiltrating immune cells (https://cistrome.shinyapps.io/timer/) (20). We analyzed the correlation of the expression of PDCD1, CTLA4 and HAVCR2 with the expression of IFNG, IL-2 and TGFB1 in HNSCC via correlation module. The gene expression level was displayed with log2 TPM. Tumor Immune Single-cell Hub (TISCH) is a scRNA-seq database focusing on tumor microenvironment. TISCH provides detailed cell-type annotation at the single-cell level, enabling the exploration of tumor microenvironment across different cancer types (http://tisch.comp-genomics.org/) (21). We explored the expression of PDCD1, CTLA4, HAVCR2, IFNG, IL-2 and TGFB1 in public data of head and neck cancer. The gene expression level was displayed with violin plot.

Statistical analysis

The data were analyzed by Graphpad 7.0 statistical software. The staining intensity of CD8, PD-1, PD-L1, CD86 and clinicopathological features of the patients was analyzed using rank-sum tests. Significant differences in tumor growth, mice weight and cell subsets were determined by using unpaired *t*-tests. *P* values <0.05 were considered statistically significant.

Results

Expression of CD8 in normal oral mucosa, OLK and OSCC tissues

Immunohistochemical staining results showed that $CD8^+$ T cells were observed in OLK and OSCC tissues (positive expression rate was 73 and 62%, respectively) and were rarely found in normal oral mucosal tissues (Supplementary Table 2, available at *Carcinogenesis* Online). The differences between normal oral mucosal tissues and OLK tissues were statistically significant ($P = 0.0006$), as well as OSCC tissues ($P < 0.0001$) (Figure 1A). In OLK tissues, the expression of CD8 was associated with smoking, drinking alcohol and the degree of abnormal epithelial dysplasia ($P = 0.0025$, $P = 0.0025$ and $P = 0.0432$) (Figure 2A). In OSCC tissues, the expression of CD8 was associated with the clinical stage and the degree of differentiation ($P = 0.0042$ and $P = 0.0429$) (Figure 3A).

Expression of PD-1 and CTLA-4 in normal oral mucosa, OLK and OSCC tissues

PD-1 immunohistochemical staining results showed that PD-1-expression could be observed in OLK and OSCC tissues (the positive expression rate was 85 and 53%, respectively), but rarely observed in normal oral mucosal tissues (Supplementary Table 2, available at *Carcinogenesis* Online). The differences between normal oral mucosal tissues and OLK tissues were statistically significant ($P = 0.0101$), as well as OSCC tissues ($P < 0.0001$). The differences between OLK and OSCC were statistically significant ($P = 0.0316$) (Figure 1B). CTLA-4 was rarely expressed in normal oral mucosa, OLK and OSCC tissues (Figure 1C). In OLK, the PD-1-expression was positively associated with the degree of epithelial hyperplasia and the PD-1-expression of lesions coming from lingual was higher than other sites (Figure 2B). In OSCC, the PD-1-expression was positively associated with the clinical stage ($P = 0.0019$) and the PD-1-expression was higher among patients with lymph node metastasis ($P = 0.0087$) (Figure 3B).

Expression of PD-L1 and CD86 in normal oral mucosa, OLK and OSCC tissues

Immunohistochemistry results showed that the expression of PD-L1 and CD86 in OLK and OSCC tissues was higher than normal oral mucosal tissues (Figure 1D and E). There was a significant difference in the expression of PD-L1 and CD86 among the three groups (normal versus OLK: $P = 0.0066$, normal versus OSCC: $P < 0.0001$, OLK versus OSCC: $P = 0.0030$). The relationship between the expression of PD-L1 and CD86 and the clinical characteristics of patients diagnosed with OLK and OSCC are described in Supplementary Table 3, available at *Carcinogenesis* Online. In OLK, the expression of PD-L1 and CD86 was higher among patients with severe epithelial dysplasia when compared with patients without epithelial dysplasia. And the expression of PD-L1 and CD86 of OLK tissues coming from lingual was higher than from gingival (Figure 2C and D). In OSCC, the expression of PD-L1 and CD86 was positively associated with the clinical stage and the degree of tumor differentiation. And the expression of PD-L1 and CD86 was higher among patients with lymph node metastasis. The CD86-expression of tumors coming from lingual was higher than gingival (Figure 3C and D).

T cells' dynamic characteristics during oral carcinogenesis *in vivo*

To clarify the dynamic changes of T cells in oral carcinogenesis, C57BL/6 were fed with tap water containing 100 μg/ml 4-NQO to construct mice models of oral carcinogenesis (Figure 4A and B). Our previous preliminary experiments showed that the isolated T cells from local lesions could not meet the requirements of flow cytometry. So, we chose spleens for further study. Spleens coming from normal (week 0), OLK (week 16) and OSCC (week 20) mice were collected to make single-cell suspensions for flow cytometry analysis. At the same time, we have verified some results of flow cytometry analysis in oral lesions by mIHC.

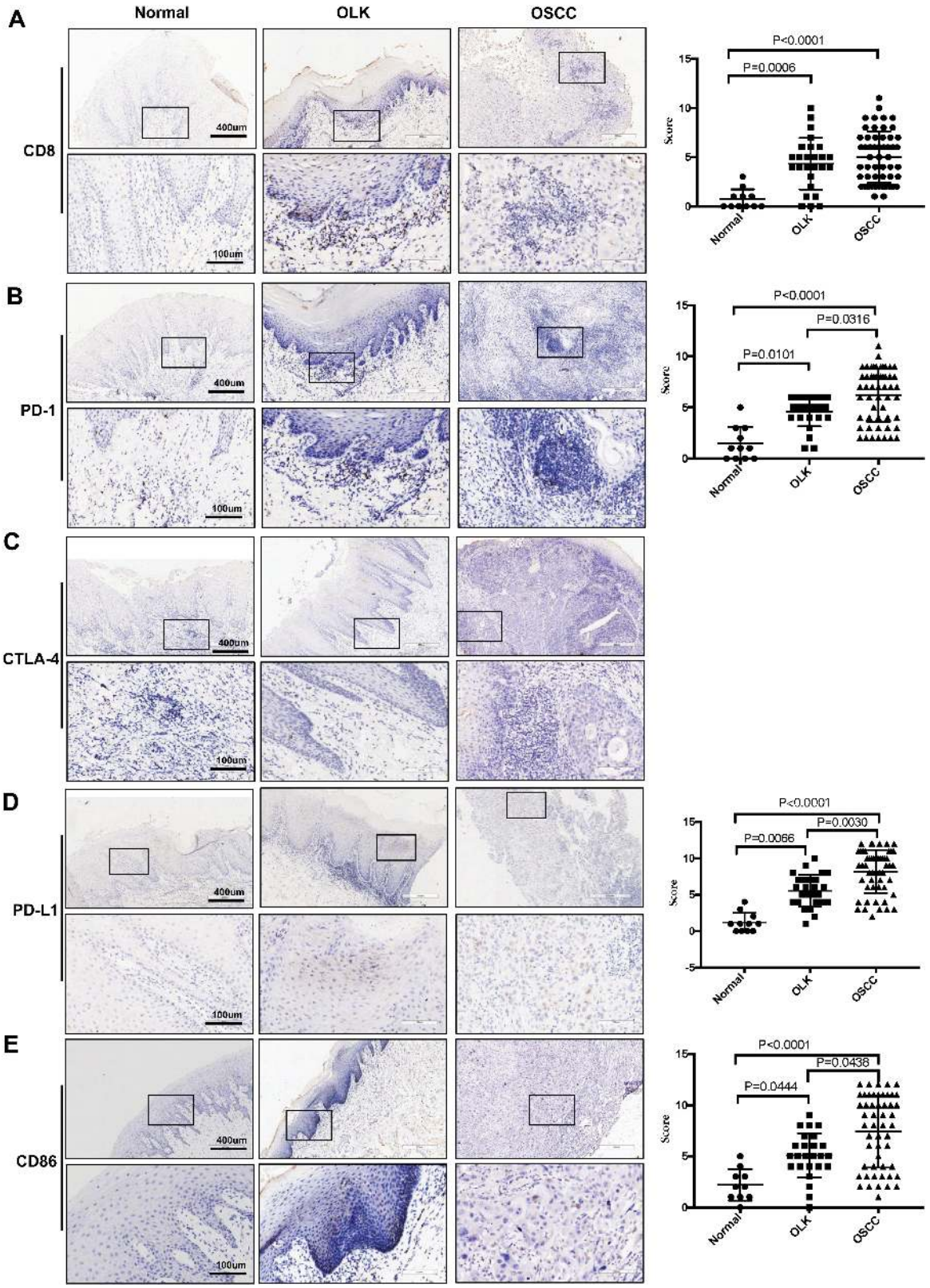

Figure 1. Immunostaining of (**A**) CD8, (**B**) PD-1, (**C**) CTLA-4, (**D**) PD-L1 and (**E**) CD86 in human normal, OLK and OSCC specimens. Immunostaining scores were analyzed by rank-sum tests.

Compared with OLK and normal mice, both for $CD4^+$ T cells and $CD8^+$ T cells, the expression of PD-1 and TIM-3 in OSCC was upregulated (Figure 4C). However, compared with normal mice, only a higher frequency of $PD\text{-}1^+CD4^+$ T cells was detected in OLK, which demonstrated the appearance of exhausted $CD4^+$ T cells was much earlier than exhausted $CD8^+$ T cells.

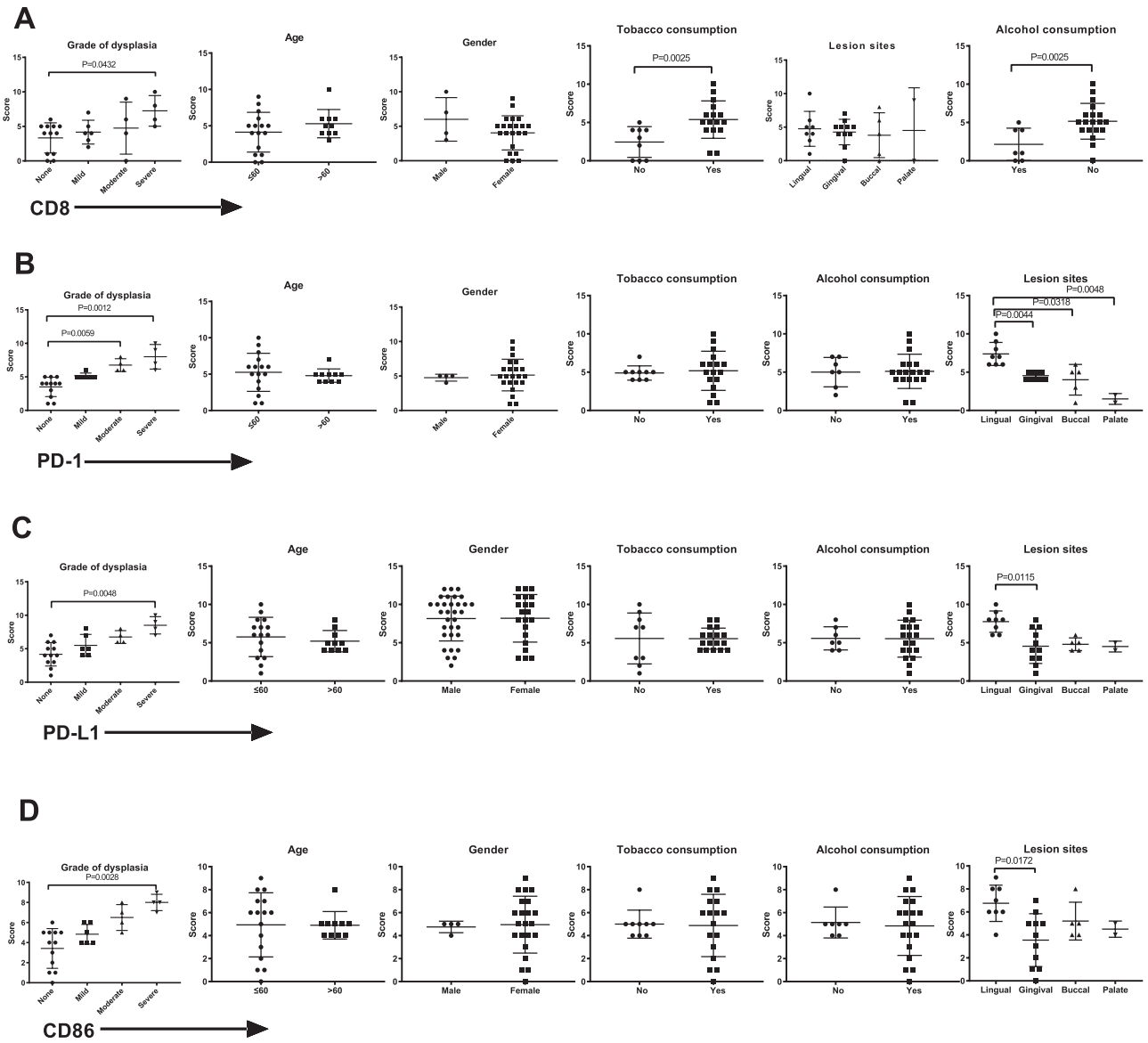

Figure 2. The relationship between the patients' clinicopathological features and the expression of (**A**) CD8, (**B**) PD-1, (**C**) PD-L1 and (**D**) CD86 in OLK.

The expression of CTLA-4$^+$CD8$^+$ T cells differed only between the normal and OSCC mice. A higher frequency of Foxp3$^+$CD4$^+$ T cells (Treg cells) was observed in OSCC (Figure 4C). An increased proportion of T-bet$^+$CD4$^+$ T cells were detected in OLK, while a higher number of EOMES$^+$CD4$^+$ T cells were observed in OSCC (Figure 4D). As for the subsets of CD8$^+$ T cells, only the proportion of EOMES$^+$CD8$^+$ T cells increased in the late stage; T-bet$^+$CD8$^+$ T cells did not change significantly throughout the entire process (Figure 4D). In the late stage, IFN-γ and TGF-β increased in T cells, but there was no significant change for IL-2 (Figure 4E). To further verify the relationship of immune checkpoint genes and cytokines, the correlation of the expression of PDCD1, CTLA4 and HAVCR2 with the expression of IFNG, IL-2 and TGFB1 in HNSCC were analyzed using the TIMER. This analysis revealed that the expression of immune checkpoint markers (PDCD1, CTLA4 and HAVCR2) was strongly positively correlated with cytokines (IFNG and IL-2), while there was no correlation between the expression of IL-2 and the expression of PDCD1, CTLA4 and HAVCR2 in HNSCC (Supplementary Figure 2A, available at *Carcinogenesis* Online). Furthermore, according to the results from TISCH webserver (tisch.comp-genomics.org) on two single-cell transcriptome datasets of human head and neck cancer (HNSC_GSE103322 and HNSC_GSE139324), exhaustion markers coexpressed with IFNG in exhausted T cells, as well as proliferative T cells (Supplementary Figure 2B, available at *Carcinogenesis* Online) (22,23). The results of mIHC demonstrated that the number of infiltrated CD4$^+$ T cells and the expression of PD-1 increased in oral carcinogenesis. Both in OLK and OSCC, the number of infiltrated CD4$^+$ T cells is significantly more than that of CD8$^+$ T cells (Figure 4F).

Efficacy of PD-1 blockade used to manage OLK *in vivo*

In the previous experiments, we found that the exhaustion of T cells mainly occurred at the stage from OLK to OSCC, so we introduced PD-1 blockade in OLK to figure out whether it could delay the progression of oral carcinogenesis. In the mice model of OLK, the rate of mice with a higher pathological grade in the PD-1 blockade group was less than that in the control group,

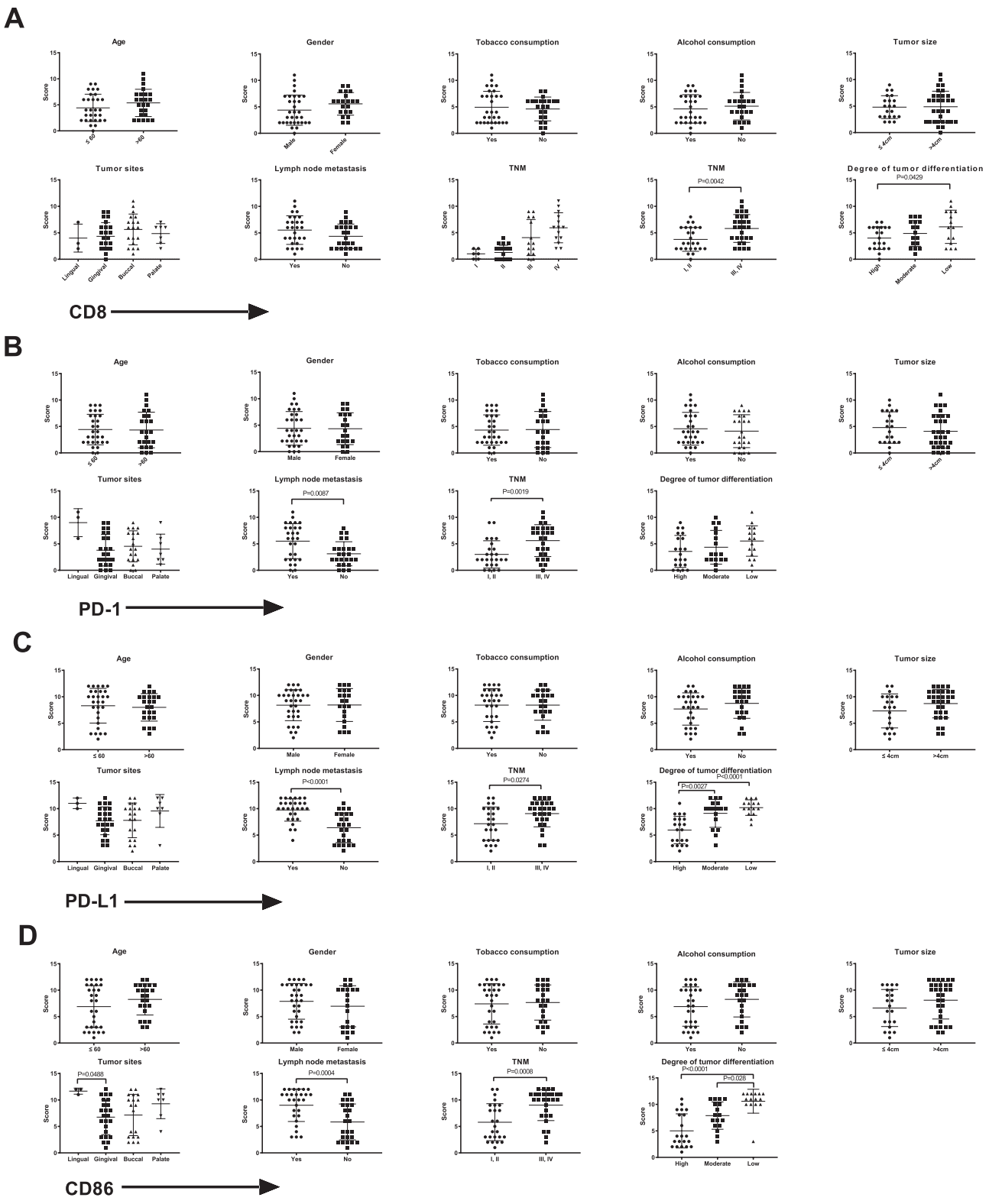

Figure 3. The relationship between the patients' clinicopathological features and the expression of (**A**) CD8, (**B**) PD-1, (**C**) PD-L1 and (**D**) CD86 in OSCC.

however, this difference was not significant (Figure 5A–C). The results of flow cytometry analysis showed a higher rate of EOMES$^+$CD8$^+$ T cells ($P < 0.05$) and IFN-γ^+CD8$^+$ T cells ($P < 0.05$) detected in the PD-1 blockade group, comparing with the control group (Figure 5D–F). The results of mIHC demonstrated that the number of infiltrated CD8$^+$ T cells increased and CD4$^+$ T cells decreased, and the expression of PD-1 decreased after PD-1 blockade (Figure 5G). These findings suggested that PD-1 blockade can active CD8$^+$ T cells to prevent the progression of oral carcinogenesis. Because of the short observation time and

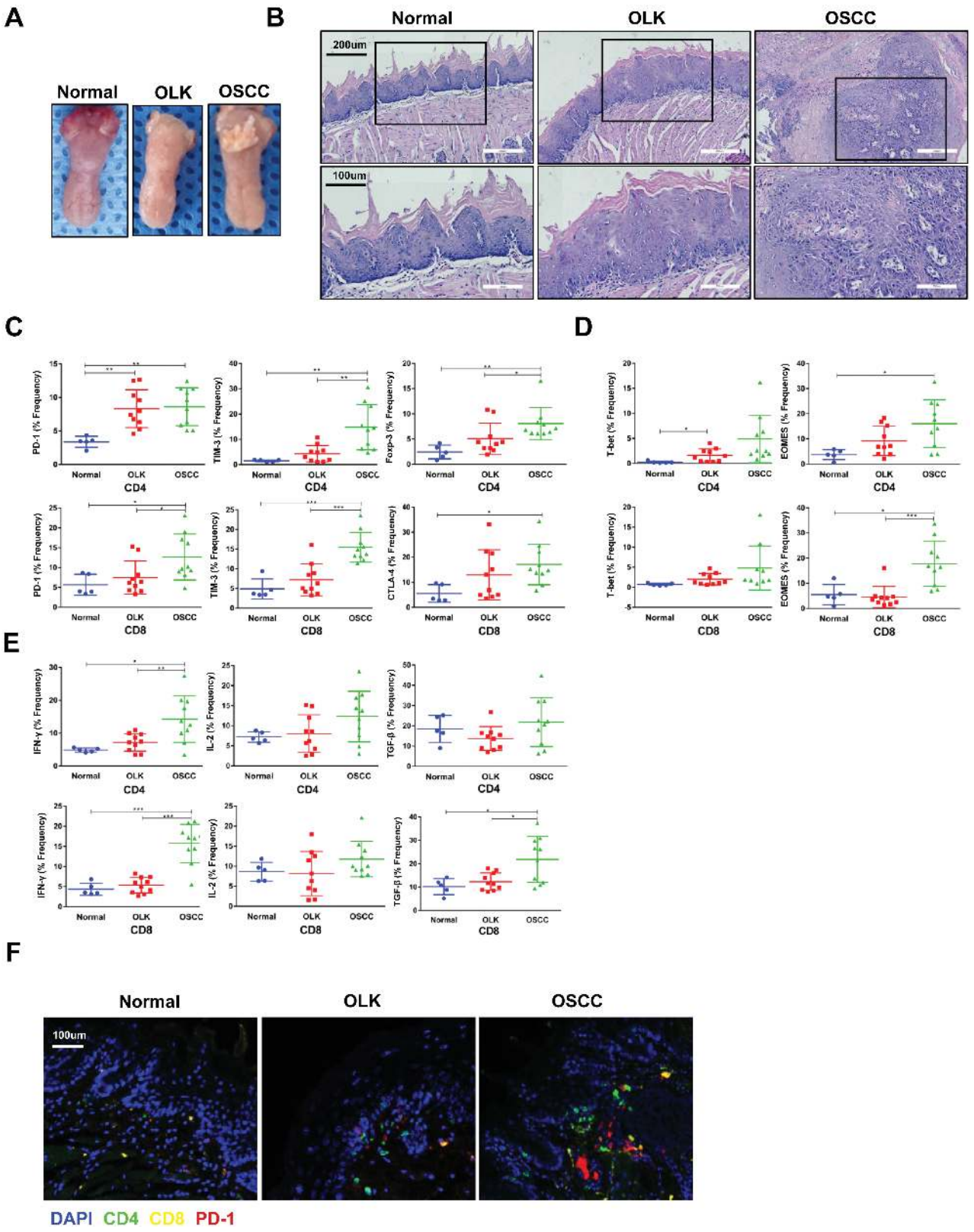

Figure 4. Dynamic characteristics of T cells in oral carcinogenesis. (**A**) Representative image of tongue visible lesions in different stages. (**B**) Representative HE staining of tongue lesions in different stages as indicated. Frequencies of (**C**) PD-1, PD-L1, TIM-3, CTLA-4, Foxp3, (**D**) T-bet, EOMES, (**E**) IFN-γ, IL-2 and TGF-β positive $CD8^+$ T cells and/or $CD4^+$ T cells in normal, OLK and OSCC mice are shown. Data are presented as the mean ± standard deviation (SD), with individual symbols representing individual mice. Significant differences in the $CD4^+$ and $CD8^+$ T cells in normal, OLK and OSCC mice were determined by unpaired *t*-test (*$P < 0.05$, **$P < 0.01$, ***$P < 0.001$). (**F**) Immunofluorescent images for CD4 (green), CD8 (yellow) and PD-1 (red) of tongue lesions from mice as indicated. The nuclei were visualized by 4′,6-diamidino-2-phenylindole (DAPI) (blue).

insufficient sample size, the efficacy of PD-1 blockade in OLK should be further studied.

Concurrent treatment with PD-1 blockade and cisplatin for the management of OSCC *in vivo*

Immunotherapy combined with chemotherapy has achieved clinical benefit in several malignancies, however, the efficacy of immunotherapy in OSCC is still unclear. Hence, we constructed OSCC mice by the 4-NQO induction treated with immune checkpoints or chemotherapy. Compared with the control group, PD-1 blockade and cisplatin significantly delayed tumor growth, both alone and in combination. We observed a remarkable reduction of tumor growth in the combination group, and no significant difference among the three experimental groups. The body weights significantly decreased in each group except for the PD-1 blockade group (Figure 6A–C).

Compared with the control group, there was a lower frequency of TIM-3$^+$CD4$^+$ T, PD-1$^+$CD8$^+$ T and TIM-3$^+$CD8$^+$ T cells in the PD-1 blockade group. These findings suggested that PD-1 blockade affected both PD-1 and TIM-3 (Figure 6D). The proportion of EOMES$^+$CD8$^+$ T cells decreased, while the proportion of T-bet$^+$CD8$^+$ T cells increased (Figure 6E. At the same time, the secretion of IFN-γ and IL-2 by both CD4$^+$ T and CD8$^+$ T cells decreased in the PD-1 blockade group (Figure 6F).

Compared with the control group, there was a lower frequency of PD-1$^+$CD4$^+$ T, and PD-1$^+$CD8$^+$ T cells, and Tregs in the cisplatin group (Figure 6D). These findings suggested that the mechanisms of cisplatin killing tumor cells may be related to the PD-1/PD-L1 pathway. Additionally, cisplatin can lower the ratio of Tregs to enhance anti-tumor immunity. The proportion of T-bet$^+$CD8$^+$ T cells increased, while that of EOMES$^+$CD8$^+$ T cells remained unchanged (Figure 6E). At the same time, the secretion of IL-2 by both CD4$^+$ T and CD8$^+$ T cells decreased in the cisplatin group (Figure 6F).

Compared with the control group, there was a lower frequency of PD-1$^+$CD4$^+$ T, and PD-1$^+$CD8$^+$ T cells in the combination group (Figure 6D). The proportion of T-bet$^+$CD8$^+$ T cells increased, while that of EOMES$^+$CD8$^+$ T and EOMES$^+$CD4$^+$ T cells decreased (Figure 6E). The secretion of IFN-γ, IL-2 and TGF-β by both CD4$^+$ T and CD8$^+$ T cells remained unchanged in the combination group (Figure 6F).

The results of mIHC demonstrated that, compared with the control group, the number of infiltrated CD8$^+$ T cells increased and CD4$^+$ T cells decreased, and the expression of PD-1 decreased whether PD-1 blockade combined with cisplatin or not. (Figure 6G).

In general, PD-1 blockade and cisplatin, either alone or in combination, had a good efficacy on the treatment of OSCC; however, there was no significant difference among the experimental groups. Moreover, mice that were not sensitive to the drugs could be found in all groups.

Discussion

In this study, we revealed that exhausted T cells played a vital role in oral carcinogenesis, which could be confirmed by the evidence from clinical specimens and the animal models. The exhaustion of T cells mainly occurred at the stage from OLK to OSCC; additionally, exhausted T cells demonstrated different characteristics at different stages. These findings were consistent with the results of previous studies (24–28).

A prominent hallmark of exhausted T cells is the persistently high expression of immunosuppressive checkpoints, such as PD-1, TIM-3 and CTLA-4 (29). Immunohistochemical results showed that the number of infiltrated CD8$^+$ T cells was positively correlated with the clinicopathological grade. Compared with normal tissues, PD-1 was highly expressed in OLK and OSCC specimens, while CTLA-4 was rarely expressed. In the subsequent animal experiments, the number of T cells isolated from lingual lesions is too small to meet the requirements of flow cytometry, so spleens were collected for further study. The expression of PD-1 on T cells increased in OLK and OSCC, while changes of CTLA-4 occurred mainly in OSCC. Also, a higher expression of PD-1 was observed in mice tongue lesions. Hence, PD-1 is of greater importance than CTLA-4 in oral carcinogenesis, especially in the early stage. Interestingly, we found that the appearance of exhausted CD4$^+$ T cells was much earlier than exhausted CD8$^+$ T cells. And the number of infiltrated CD4$^+$ T cells is more than CD8$^+$ T cells in mice tongue lesions. Additionally, there was a higher frequency of Tregs detected in oral carcinogenesis. These findings suggested that CD4$^+$ T cells had a crucial influence on regulating the progression of oral carcinogenesis. A study on oral tongue squamous cell carcinoma emphasized the importance of CD4$^+$ T cells in tumors as pivotal regulators of PD-L1 levels and determined the factors related to the outcomes associated with PD-1 blockade therapy (25). In our study, however, the efficacy of the introduced PD-1 blockade in OLK mice was not significant. PD-1 blockade used alone in OSCC can delay tumors' growth, however, we found there are a few mice that respond badly to PD-1 blockade in our preliminary study. And in these mice, tumors are mostly exogenous, and the number of infiltrated T cells is quite small. How to turn the 'cold' tumor to be 'hot' to respond well to PD-1 blockade? Cisplatin is a classical chemotherapy drug to manage OSCC in clinical. It can kill cancer cells and recruit immune cells to make the tumor become 'hot'. Compared with the monotherapy group, we did observe that the tumor sizes of some mice in the combined group was significantly reduced, although this difference could not be reflected in the statistical data. In OSCC, we observed that the expression of PD-1 and TIM-3 in the experimental groups decreased, suggesting that lower expression of suppressive immune checkpoints may indicate good outcomes. Ngiow *et al.* determined that the expression of PD-1 on tumor-infiltrating CD8$^+$ T cells was lower in sensitive tumors than resistible tumors (19). Another study showed that the dysfunction in tumor-infiltrating PD-1^{high}CD8$^+$ T cells (completely exhausted CD8$^+$ T cells) could not be reversed by PD-1 blockade; only the dysfunction of PD-1^{low} CD8$^+$ T cells (partially exhausted CD8$^+$ T cells) could be reversed by blockade (30). In the cisplatin group, the changed expression of PD-1 revealed that the mechanisms of cisplatin to kill tumor cells may be related to the PD-1/PD-L1 pathway. Chemotherapy can induce local immune suppression in resistible tumors through PD-L1 upregulation (31–34). Thus, concurrent treatment of chemotherapy and PD-1 blockade may improve antitumor response.

Another characteristic of exhausted T cell is the altered expression of transcription factors, such as EOMES and T-bet (35). EOMES and T-bet mainly regulate the effector T cell's function and memory formation. T-bet^{hi} CD8$^+$ T cells retaining polyfunctionality can persist for long durations and differentiate into EOMES^{hi} CD8$^+$ T cells. While EOMES^{hi} T cells are terminal cells that are prone to apoptosis, however, they can secrete cytokines (such as IFN-γ) and granzyme B to kill target cells (36). Thus, both T-bet^{hi} T cells and EOMES^{hi} T cells play an important role in the control of tumors. A higher proportion of T-bet$^+$CD4$^+$ T cells was detected in the early stage, while an increased proportion of EOMES$^+$CD8$^+$ T cells were detected in the late stage. A study on a murine liver cancer model suggested

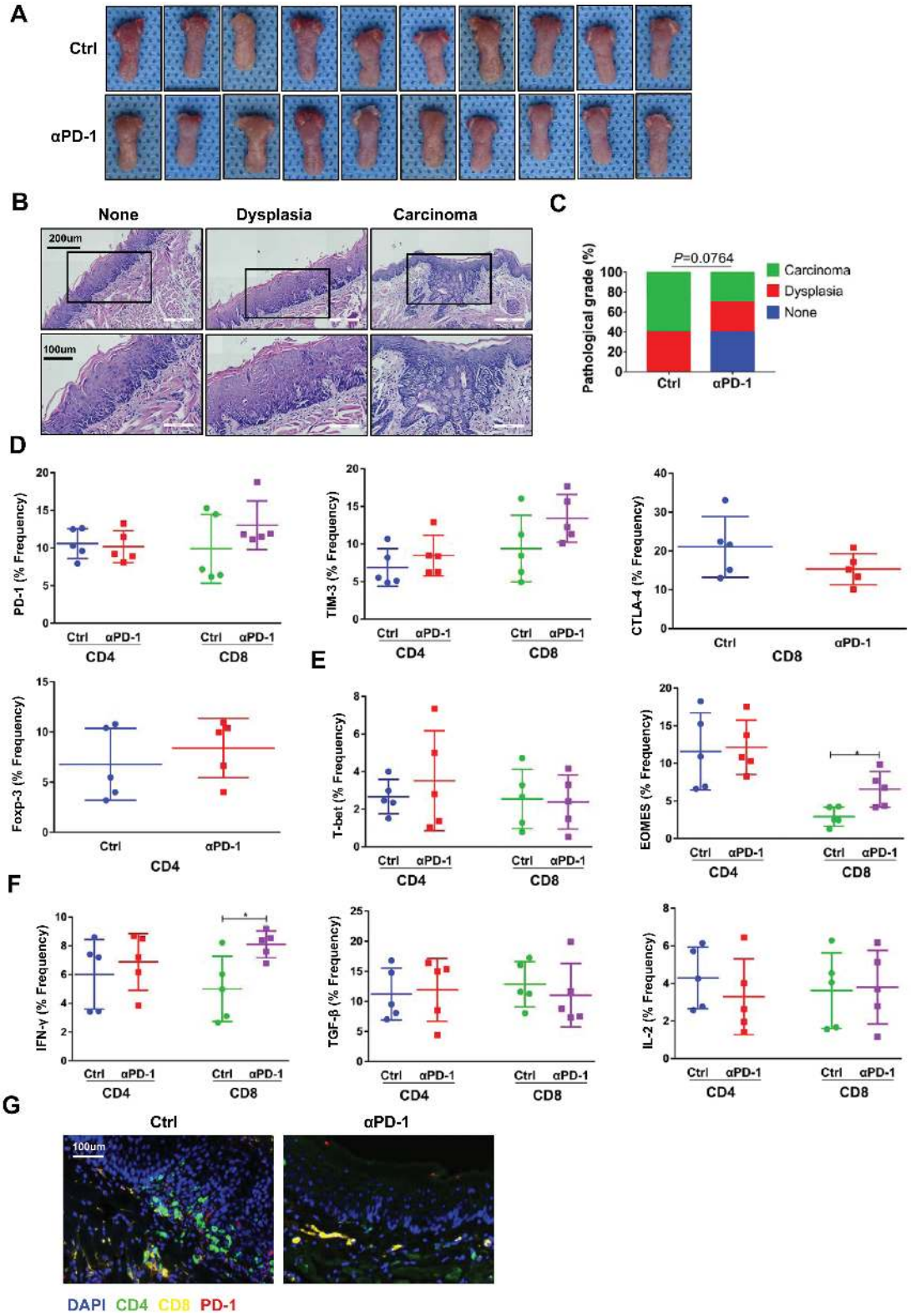

Figure 5. Characteristics of T cells in different groups when PD-1 blockade used to manage OLK *in vivo*. (**A**) Images of tongue visible lesions in different treatment groups as indicated. (**B**) Representative HE staining of tongue lesions in different treatment groups as indicated (none: without dysplasia). (**C**) Quantification of pathological grades in different treatment groups. The data were analyzed by the Cochran–Armitage test. (**D–F**) Frequencies of PD-1, PD-L1, TIM-3, CTLA-4, Foxp3, T-bet, EOMES, IFN-γ, IL-2 and TGF-β positive $CD8^+$ T cells and/or $CD4^+$ T cells in different treatment groups. Data are presented as the mean ± standard deviation (SD), with individual symbols representing individual mice. Significant differences in the $CD4^+$ and $CD8^+$ T cells in different treatment groups were determined by unpaired *t*-test (*$P < 0.05$, **$P < 0.01$, ***$P < 0.001$). (**G**) Representative immunofluorescent images for CD4 (green), CD8 (yellow) and PD-1 (red) of tongue lesions in different treatment groups as indicated. The nuclei were visualized by DAPI (blue).

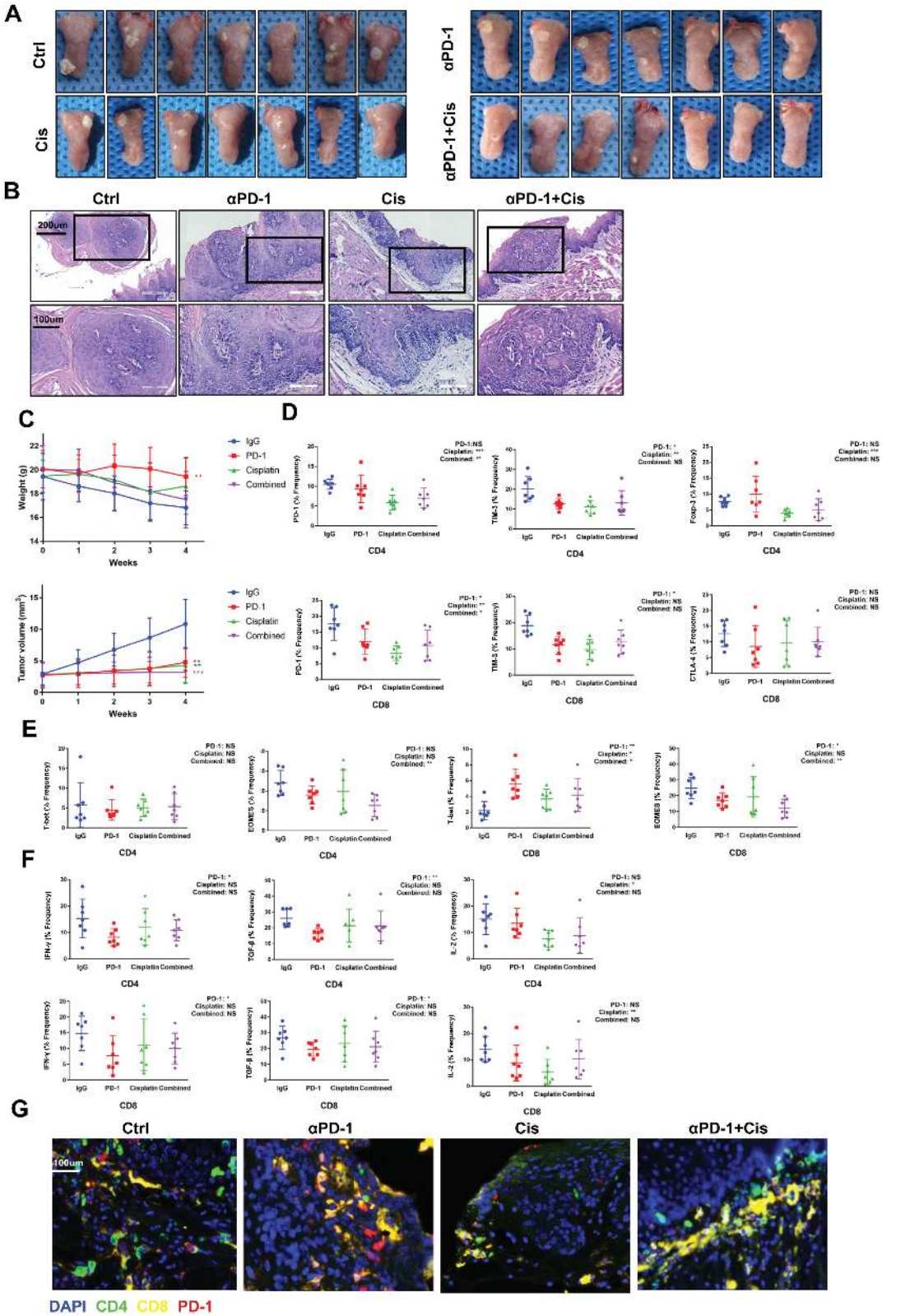

Figure 6. PD-1 blockade combined with or without cisplatin for the control of OSCC *in vivo*. (**A**) Images of tongue visible lesions in different treatment groups as indicated. (**B**) Representative HE staining of tongue lesions in different treatment groups as indicated. (**C**) Tumor sizes and body weight are presented as mean ± SEM. Significant differences in tumor growth and body weight in the different groups were determined using a Mann–Whitney test (*$P < 0.05$, **$P < 0.01$, ***$P < 0.001$). (**D–F**) Frequencies of PD-1, PD-L1, TIM-3, CTLA-4, Foxp3, T-bet, EOMES, IFN-γ, IL-2 and TGF-β positive $CD8^+$ T cells and/or $CD4^+$ T cells in different treatment groups. Data are presented as the mean ± standard deviation (SD), with individual symbols representing individual mice. Significant differences in the $CD4^+$ and $CD8^+$ T cells in different treatment groups were determined by unpaired *t*-test (*$P < 0.05$, **$P < 0.01$, ***$P < 0.001$). (**G**) Representative immunofluorescent images for CD4 (green), CD8 (yellow) and PD-1 (red) of tongue lesions in different treatment groups as indicated. The nuclei were visualized by DAPI (blue).

that T cells are with a high expression of EOMES in the early stage, however, the expression of T-bet and EOMES both reduced over the course of tumor progression (37). Another study determined that progenitor exhausted T cells with high expression of T-bet and low expression of EOMES had the potential to be reinvigorated by PD-1 blockade in both cancers and chronic viral infections (38). Our findings revealed that PD-1 blockade could increase the rate of $EOMES^{+}CD8^{+}$ T cells ($P < 0.05$); this could be a strong motivation for the introduction of PD-1 blockade in OLK. In our mice models of OSCC, the expression of T-bet increased and EOMES decreased in the experiment groups; this was conducive to the stable control of tumors. Therefore, the expression of T-bet and EOMES could be potential indicators of the efficacy of PD-1 blockade.

Additionally, the ability of exhausted T cells to secrete cytokines changed. Previous studies suggested that cytokines, such as IFN-γ, IL-2 and TGF-β, were either helpful or harmful for tumor control; however, there is a growing body of evidence suggesting that cytokines could both limit and promote the progression of tumors (39). Our study found, compared with normal and OLK mice, a higher secretion of IFN-γ and TGF-β was observed in OSCC mice. Subsequent results based on TCGA database and single-cell transcriptome datasets also showed the expression of cytokines (IFNG and IL-2) were positively correlated with the expression of immune checkpoint markers (PDCD1, CTLA4 and HAVCR2) in HNSCC. These results demonstrated that exhausted T subsets were with a high expression level of some cytokines. When drugs were introduced in OSCC mice, the secretion of IFN-γ and IL-2 decreased in the experimental groups. Terminal exhausted T cells ($EOMES^{+}$ T cells) overly secreting cytokines, such as IFN-γ, are more prone to apoptosis than the progenitor exhausted T cells ($T\text{-}bet^{hi}$ T cells) (40,41). When the tumor antigen persists, the former continues to differentiate into the latter as a supplement to kill tumor cells, which can cause the progenitor subsets to be depleted. Optimal immune stimulation intensity is vital to the immunotherapy strategy, so persistently high levels of cytokines were not conducive to OSCC control.

In summary, exhausted T cells were closely related to oral carcinogenesis and the exhausted T cells were with dynamic characteristics. PD-1 blockade demonstrated a certain potential in delaying the progression from OLK to OSCC, but its exact efficacy needed to be further confirmed. PD-1 blockade combined with/without cisplatin showed a good curative effect in OSCC, and T cells' status and reasonable immunotherapy strategies are the keys to fulfill the successful tumor control. Our studies provide a strong theoretical basis for the usage of PD-1 blockade combined with/without cisplatin to manage oral precancer or OSCC in clinical. Further studies are needed to identify the characteristics of patients who are sensitive to PD-1 blockade combined with/without cisplatin, and finally, personalized scenarios are made to maintain lasting tumor control.

Supplementary material

Supplementary data are available at *Carcinogenesis* online.

Supplementary Figure 1. The flow chart of the whole experimental design. (**A**) Immunohistochemical markers of clinical specimens. (**B**) The flow chart of animal experimental design. (**C**) Flow cytometry gating strategies.

Supplementary Figure 2. TIMER and TISCH database analysis. (**A**) Immune checkpoint genes are correlated with cytokines in HNSCC. The gene expression level was displayed with log2 TPM. (**B**) Distribution of expression of PDCD1, CTLA4, HAVCR2, IFNG, IL-2 and TGFB1 in different cell types across datasets in HNSCC (violin plot).

Funding

This work was supported by grants from National Natural Science Foundation of China (81771086, 81470747, 81972551), China Postdoctoral Science Foundation (2019T120863) and the CAMS Innovation Fund for Medical Sciences (CIFMS, 2019-I2M-5-004). The funding agencies had no role in the study design, collection, analysis or interpretation of data, writing of the report or the decision to submit the article for publication.

Conflict of Interest Statement: The authors declared no conflict of interest.

References

1. Warnakulasuriya, S. (2010) Living with oral cancer: epidemiology with particular reference to prevalence and life-style changes that influence survival. *Oral Oncol.*, 46, 407–410.
2. Chi, A.C. *et al.* (2015) Oral cavity and oropharyngeal squamous cell carcinoma—an update. *CA Cancer J. Clin.*, 65, 401–421.
3. Warnakulasuriya, S. *et al.* (2016) Malignant transformation of oral leukoplakia: a systematic review of observational studies. *J. Oral Pathol. Med.*, 45, 155–166.
4. Wherry, E.J. (2011) T cell exhaustion. *Nat. Immunol.*, 12, 492–499.
5. Ramachandran, P. *et al.* (2019) Resolving the fibrotic niche of human liver cirrhosis at single-cell level. *Nature*, 575, 512–518.
6. Chen, D.S. *et al.* (2017) Elements of cancer immunity and the cancer-immune set point. *Nature*, 541, 321–330.
7. Singer, M. *et al.* (2016) A distinct gene module for dysfunction uncoupled from activation in tumor-infiltrating T cells. *Cell*, 166, 1500–1511.e9.
8. Bretscher, P.A. (1999) A two-step, two-signal model for the primary activation of precursor helper T cells. *Proc. Natl. Acad. Sci. USA*, 96, 185–190.
9. Pauken, K.E. *et al.* (2016) Epigenetic stability of exhausted T cells limits durability of reinvigoration by PD-1 blockade. *Science*, 354, 1160–1165.
10. Balar, A.V. *et al.*; IMvigor210 Study Group. (2017) Atezolizumab as first-line treatment in cisplatin-ineligible patients with locally advanced and metastatic urothelial carcinoma: a single-arm, multicentre, phase 2 trial. *Lancet*, 389, 67–76.
11. Borghaei, H. *et al.* (2015) Nivolumab versus docetaxel in advanced nonsquamous non-small-cell lung cancer. *N. Engl. J. Med.*, 373, 1627–1639.
12. Ribas, A. *et al.* (2016) Association of pembrolizumab with tumor response and survival among patients with advanced melanoma. *JAMA*, 315, 1600–1609.
13. Lin, W. *et al.* (2018) Crosstalk between PD-1/PD-L1 blockade and its combinatorial therapies in tumor immune microenvironment: a focus on HNSCC. *Front. Oncol.*, 8, 532.
14. Ueno, M. *et al.* (2019) Nivolumab alone or in combination with cisplatin plus gemcitabine in Japanese patients with unresectable or recurrent biliary tract cancer: a non-randomised, multicentre, open-label, phase 1 study. *Lancet Gastroenterol. Hepatol.*, 4, 611–621.
15. Zhou, Y. *et al.* (2018) Immune-checkpoint inhibitor plus chemotherapy versus conventional chemotherapy for first-line treatment in advanced non-small cell lung carcinoma: a systematic review and meta-analysis. *J. Immunother. Cancer*, 6.
16. Lodi, G. *et al.* (2016) Interventions for treating oral leukoplakia to prevent oral cancer. *Cochrane Database Syst. Rev.*, 7, CD001829.
17. Patsoukis, N. *et al.* (2014) PD-1 inhibits T cell proliferation by upregulating p27 and p15 and suppressing Cdc25A. *Cell Cycle*, 11, 4305–4309.
18. Tran, L. *et al.* (2017) Cisplatin alters antitumor immunity and synergizes with PD-1/PD-L1 inhibition in head and neck squamous cell carcinoma. *Cancer Immunol. Res.*, 5, 1141–1151.
19. Ngiow, S.F. *et al.* (2015) A threshold level of intratumor CD8+ T-cell PD1 expression dictates therapeutic response to anti-PD1. *Cancer Res.*, 75, 3800–3811.
20. Li, T. *et al.* (2017) TIMER: a web server for comprehensive analysis of tumor-infiltrating immune cells. *Cancer Res.*, 77, e108–e110.
21. Sun, D. *et al.* (2021) TISCH: a comprehensive web resource enabling interactive single-cell transcriptome visualization of tumor microenvironment. *Nucleic Acids Res.*, 49, D1420–D1430.

22. Puram, S.V. *et al*. (2017) Single-cell transcriptomic analysis of primary and metastatic tumor ecosystems in head and neck cancer. *Cell*, 171, 1611–1624.e24.
23. Cillo, A.R. *et al*. (2020) Immune landscape of viral- and carcinogen-driven head and neck cancer. *Immunity*, 52, 183–199.e9.
24. Wang, Z. *et al*. (2019) Syngeneic animal models of tobacco-associated oral cancer reveal the activity of in situ anti-CTLA-4. *Nat. Commun.*, 10, 5546.
25. Wang, J. *et al*. (2017) PD-1 blockade prevents the development and progression of carcinogen-induced oral premalignant lesions. *Cancer Prev. Res. (Phila)*., 10, 684–693.
26. Chen, Y. *et al*. Blockade of PD-1 effectively inhibits in vivo malignant transformation of oral mucosa. *OncoImmunology*, 7, 1.
27. Wen, L. *et al*. (2019) Contributions of T cell dysfunction to the resistance against anti-PD-1 therapy in oral carcinogenesis. *J. Exp. Clin. Cancer Res*., 38, 299.
28. Jia, L. *et al*. (2020) BMI1 inhibition eliminates residual cancer stem cells after PD1 blockade and activates antitumor immunity to prevent metastasis and relapse. *Cell Stem Cell*, 27, 238–253.e6.
29. Thommen, D.S. *et al*. (2018) T cell dysfunction in cancer. *Cancer Cell*, 33, 547–562.
30. Kansy, B.A. *et al*. (2017) PD-1 status in CD8+ T cells associates with survival and anti-PD-1 therapeutic outcomes in head and neck cancer. *Cancer Res*., 77, 6353–6364.
31. Peng, J. *et al*. (2015) Chemotherapy induces programmed cell death-ligand 1 overexpression via the nuclear factor-κB to foster an immunosuppressive tumor microenvironment in ovarian cancer. *Cancer Res*., 75, 5034–5045.
32. Wang, N. *et al*. (2019) Loss of Scribble confers cisplatin resistance during NSCLC chemotherapy via Nox2/ROS and Nrf2/PD-L1 signaling. *EBioMedicine*, 47, 65–77.
33. Shen, M. *et al*. (2019) Inhibition of ATM reverses EMT and decreases metastatic potential of cisplatin-resistant lung cancer cells through JAK/STAT3/PD-L1 pathway. *J. Exp. Clin. Cancer Res*., 38, 149.
34. Zhang, P. *et al*. (2016) Upregulation of programmed cell death ligand 1 promotes resistance response in non-small-cell lung cancer patients treated with neo-adjuvant chemotherapy. *Cancer Sci*., 107, 1563–1571.
35. Paley, M.A. *et al*. (2012) Progenitor and terminal subsets of CD8+ T cells cooperate to contain chronic viral infection. *Science*, 338, 1220–1225.
36. Intlekofer, A.M. *et al*. (2005) Effector and memory CD8+ T cell fate coupled by T-bet and eomesodermin. *Nat. Immunol*., 6, 1236–1244.
37. Schietinger, A. *et al*. (2016) Tumor-specific T cell dysfunction is a dynamic antigen-driven differentiation program initiated early during tumorigenesis. *Immunity*, 45, 389–401.
38. Miller, B.C. *et al*. Subsets of exhausted CD8+ T cells differentially mediate tumor control and respond to checkpoint blockade. *Nat. Immunol*., 20, 326–336.
39. Batlle, E.M.J. (2019) Transforming growth factor-b signaling in immunity and cancer. *Immunity,* 50, 924–940.
40. Jansen, C.S. *et al*. (2019) An intra-tumoral niche maintains and differentiates stem-like CD8 T cells. *Nature*, 576, 465–470.
41. Pai, C.S. *et al*. (2019) Clonal deletion of tumor-specific T cells by interferon-γ confers therapeutic resistance to combination immune checkpoint blockade. *Immunity*, 50, 477–492.